Storing Optical Information as a Mechanical Excitation in a Silica Optomechanical Resonator

Victor Fiore,[1] Yong Yang,[1] Mark C. Kuzyk,[1] Russell Barbour,[1] Lin Tian,[2] and Hailin Wang[1]
[1]Department of Physics, University of Oregon, Eugene, Oregon 97403, USA
[2]Department of Physics, University of California, Merced, California 95343, USA
(Received 31 May 2011; published 19 September 2011)

We report the experimental demonstration of storing optical information as a mechanical excitation in a silica optomechanical resonator. We use writing and readout laser pulses tuned to one mechanical frequency below an optical cavity resonance to control the coupling between the mechanical displacement and the optical field at the cavity resonance. The writing pulse maps a signal pulse at the cavity resonance to a mechanical excitation. The readout pulse later converts the mechanical excitation back to an optical pulse. The storage lifetime is determined by the relatively long damping time of the mechanical excitation.

DOI: 10.1103/PhysRevLett.107.133601 PACS numbers: 42.50.Wk, 03.67.Hk, 07.10.Cm

Light is a natural and ideal information carrier, but is difficult to store. Light storage is important for all-optical information networks and is also an essential ingredient for long-distance quantum communication [1,2]. A variety of approaches for light storage have been actively pursued. Storage of light as spin excitations in atomic media or as persistent atomic excitations in inhomogeneously broadened solids has been realized in quantum as well as classical regimes [3–6]. Optical pulses have also been stored in dynamically tunable coupled-resonator optical waveguides or as acoustic excitations in optical fibers [7–10].

Optomechanical resonators, in which optical fields couple to mechanical oscillations via radiation pressure [see Fig. 1(a)], provide another potential avenue for light storage. Optomechanical interactions have been successfully explored for the control of mechanical as well as optical processes in these resonators in the steady state [11]. Earlier experimental studies have demonstrated optomechanical parametric amplification, laser cooling, and normal mode splitting of a mechanical mode [12–18]. Optomechanical processes analogous to the well-known phenomenon of electromagnetically induced transparency (EIT) have also been realized recently in both optical and microwave regimes [19–21].

Here, we report a proof-of-principle experimental demonstration of storing optical information as a mechanical excitation in a silica resonator via transient optomechanical processes, with the storage lifetime determined by the relatively long decay time of the mechanical excitation. In comparison with atomic or spin systems, an optomechanical resonator features the remarkable property that an optically active mechanical mode can couple to any of the optical resonances via radiation pressure. Optomechanical processes not only can store light at a given wavelength as a mechanical excitation, but also can map the stored mechanical excitation back to light at practically any desired wavelength [22–25]. This capability of wavelength conversion can play a special role in both classical and quantum networks, for example, by converting optical information from a given wavelength, including microwaves, to a wavelength that is suitable for long-distance communication, or by mapping photons emitted from one type of quantum system to photons that can couple to another type of quantum system. In comparison with light storage as acoustic waves in an optical fiber [10], mechanical oscillators with high Q factors can lead to a storage lifetime much longer than that can be achieved with Brillouin-scattered sound waves in a fiber.

For optomechanical light storage, we use ''writing'' and ''readout'' laser pulses tuned to one mechanical frequency,

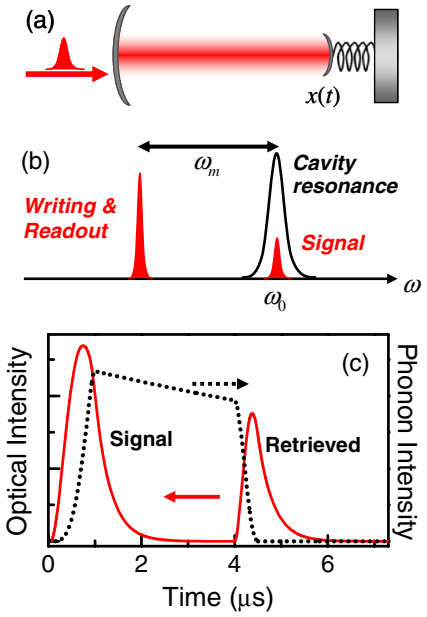

FIG. 1 (color online). (a) Schematic of an optomechanical resonator. (b) Spectral position for the writing, readout, and signal pulses. (c) The intensity of intracavity signal and retrieved pulses (solid red line), along with the intensity of the stored mechanical oscillation (dotted black line), as a function of time, illustrating the optomechanical process of light storage and retrieval.

ω_m, below the optical cavity resonance to control the coupling between the mechanical displacement and the optical field at the cavity resonance [see Fig. 1(b)]. The writing pulse maps a signal pulse at the cavity resonance to a mechanical excitation. The readout pulse later converts the mechanical excitation back to an optical pulse at the cavity resonance. As illustrated in Fig. 1(a), in an optomechanical resonator, the displacement of a mechanical oscillator modulates the frequency of an optical cavity mode, with $\omega_c(x) = \omega_0 + gx$, where x is the mechanical displacement and g is the optomechanical coupling coefficient. In the limit that $\omega_m \gg \kappa$ (the resolved sideband limit) and $n_c \gg 1$ where κ is the cavity decay rate and n_c is the intracavity photon number for either the writing or the readout pulse, the interaction between the mechanical displacement and the optical field at the cavity resonance can be approximated as a coupled oscillator system, with an effective interaction Hamiltonian given by $H_{\rm int} = \hbar G(\hat{a}^+\hat{b} + \hat{a}\hat{b}^+)$, where $\hat{a}$ and $\hat{b}$ are the annihilation operators for the optical field and the mechanical displacement, respectively, and $G = gx_{\rm zpf}\sqrt{n_c}$ is the effective optomechanical coupling rate with $x_{\rm zpf}$ being the zero-point fluctuation for the mechanical mode [22]. For this system, the writing and readout pulses can control or switch on or off the effective optomechanical coupling between the optical field and the mechanical displacement. As shown in Fig. 1(c), for the storage process, a writing pulse couples a signal pulse to the mechanical mode, generating a mechanical excitation. For the retrieval process, a readout pulse couples the stored mechanical excitation to the cavity mode, mapping the mechanical excitation back to an optical pulse. Note that the optomechanical storage and retrieval processes can not only preserve the phase coherence, but also in principle the quantum state of light [22].

We used silica microspheres as a model system for an optomechanical resonator [18]. Deformed silica microspheres with a deformation near 2% and a diameter near 30 μm were fabricated by fusing together two nondeformed microspheres of similar sizes with a CO_2 laser. The small deformation enables free-space evanescent excitation of whispering gallery modes (WGMs) near the sphere equator, with a coupling efficiency of 9% under resonant excitation. A breathing mode of the sphere with $(n, l) = (1, 2)$, where n and l are the radial and angular mode numbers, respectively, was used as the mechanical oscillator. For the experiments presented in this Letter, $\omega_m/2\pi = 108.4$ MHz, $\gamma_m/2\pi = 38$ kHz, and $\kappa/2\pi = 40$ MHz, corresponding to a mechanical Q factor near 3000 and an optical finesse near 0.5×10^5, as determined from displacement power spectra and optical transmission spectra.

The writing, readout, and signal pulses with a wavelength near 800 nm were all derived from the same laser beam generated from a tunable Ti:Sapphire ring laser. The writing and readout pulses, with the same frequency, ω_l, were obtained by gating the laser beam with an acousto-optic modulator (AOM). The laser pulses propagated through an electro-optic modulator (EOM), with the electro-optic phase modulation synchronized with the writing pulse (there is no phase modulation for the readout pulse). The higher frequency sideband generated by the phase modulation served as the signal pulse. The frequency of the signal pulse, ω_s, is locked to a given WGM resonance with a Pound-Drever-Hall technique. The timing and temporal profile of the signal pulse is the same as those of the writing pulse. The intracavity peak power of the signal pulse is kept below a few percent of that of the writing and readout pulses. Unless otherwise specified, we set the EOM modulation frequency to ω_m such that $\omega_l = \omega_s - \omega_m$ and have used the pulse sequence shown in the inset of Fig. 2(a). All experiments were carried out at room temperature.

Incident writing and readout pulses were also used as the local oscillator for the heterodyne detection of signal and retrieved pulses emitted from the optical resonator, respectively. Since the signal pulse is generated directly

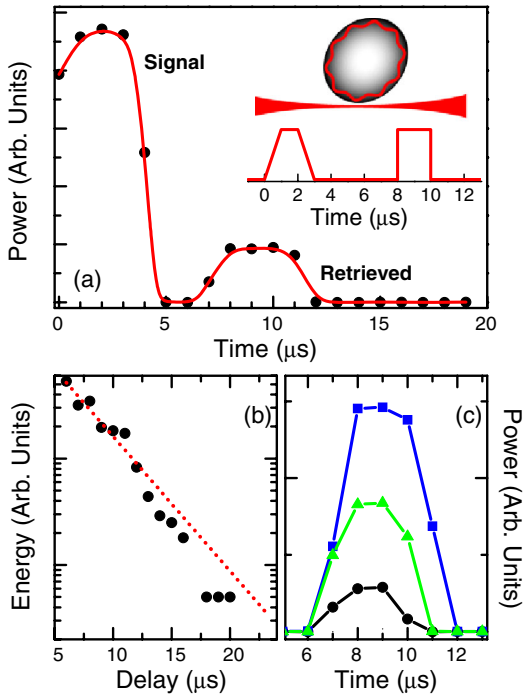

FIG. 2 (color online). (a) The power of the heterodyne-detected signal and retrieved pulses emitted from the resonator as a function of time. The solid curve serves as a guide to the eye. The inset illustrates free-space evanescent excitation of a WGM and the timing of the writing and readout pulses used for the experiment. (b) Retrieved pulse energy as a function of the delay between the readout (3 μs in duration) and writing pulses. An exponential fit shown as the red dotted line yields a storage lifetime of 3.5 μs. (c) The temporal profile of the retrieved pulse generated by a readout pulse with duration of 0.3, 0.6, 1.4 μs (from bottom to top), under otherwise identical conditions as those for (a).

from the writing pulse with an electro-optic phase modulation, the heterodyne detection is not sensitive to the part of the signal pulse that is not emitted from the optical resonator. A spectrum analyzer in a time-gated detection mode was used for time-resolved heterodyne detection, with the time resolution limited by the resolution bandwidth (1 MHz) as well as the gate length (3 μs). More experimental details along with a diagram for the experimental setup are described in the Supplemental Material [26].

Figure 2 presents a proof-of-principle experimental demonstration of optomechanical light storage. Figure 2(a) shows the heterodyne-detected signal and retrieved pulses emitted from the silica resonator. In this experiment, the readout pulse, which arrives 6.5 μs after the center of the signal pulse, interacts with the mechanical excitation induced by the signal and the writing pulse, generating the retrieved pulse. The incident writing and readout pulses produce an estimated intracavity photon number of $n_c = 1.5 \times 10^6$, corresponding to a peak optomechanical coupling rate of $G_0/2\pi = 2$ MHz. To determine the light storage lifetime, we plot in Fig. 2(b) the energy of the retrieved pulse, obtained from measurements similar to those shown in Fig. 2(a), as a function of the delay between the writing and the readout pulse. The pulse energy decays exponentially as a function of the delay, yielding a storage lifetime of 3.5 μs, which is in good agreement with the mechanical linewidth, $\gamma_m/2\pi = 38$ kHz, obtained from the displacement power spectrum.

The temporal profiles of the signal and retrieved pulses shown in Fig. 2(a) are significantly modified by the time resolution of the heterodyne detection measurement and by the temporal profile of the local oscillators (i.e., the writing and readout pulses). Figure 2(c) shows the heterodyne-detected retrieved pulse with the durations of the readout pulse increasing incrementally from 0.3 μs to 1.4 μs, indicating that the time resolution of the heterodyne measurement is approximately 3 μs. The powers obtained in these transient measurements are effectively the average power over a given detection period.

Optomechanical storage and retrieval processes are characterized by their distinct dependence on the intensity of the writing and readout pulses and on the detuning between ω_s and ω_l. Figure 3(a) shows the dependence of the retrieved pulse energy on the relative readout intensity, I/I_0, with I_0 corresponding to $G_0/2\pi = 0.7$ MHz. Similar highly nonlinear dependence was also observed when the writing intensity was varied. Figure 3(b) shows the retrieved pulse energy as a function of the detuning between ω_s and ω_l at two different readout intensities, with ω_s remaining locked to the cavity resonance. For Figs. 3(a) and 3(b), the writing intensity is fixed at I_0 and the duration of the readout pulse is 3 μs. The observed resonance in Fig. 3(b) centered at $\omega_s - \omega_l = \omega_m$ confirms the optomechanical origin of the light storage and retrieval processes. As shown in Fig. 3(b), the spectral line shape observed is independent of the intensity of the readout pulse. The same spectral line shape was also observed at higher readout intensities.

The experimental results in Figs. 2 and 3 are in good agreement with the theoretical calculation, for which we used the coupled oscillator equations to describe the optomechanical coupling between the mechanical displacement and the optical field at the cavity resonance (see [26]), with all parameters determined by the experiments. Figure 3(c) shows the calculated intracavity intensity for both the signal and the retrieved pulse, along with the intensity of the stored mechanical oscillation, as a function of time under the conditions of the experiment shown in Fig. 2(a). Although the temporal profiles of the pulses are significantly modified in the experiment due to the limited time resolution as well as the temporal profile of the local oscillators, the relative pulse energy obtained in the experiment agrees well with the theoretical expectation. Figure 3(c) also indicates that the small signal-to-retrieval conversion efficiency observed is to a large degree due to the decay of the mechanical excitation, since the delay

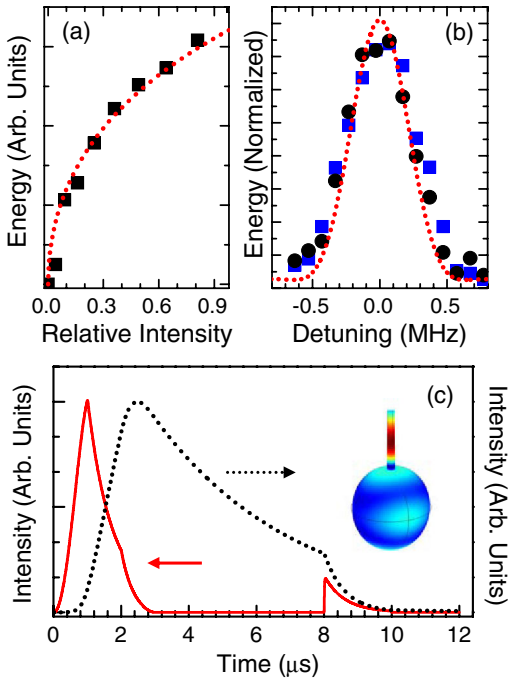

FIG. 3 (color online). (a) Retrieved pulse energy as a function of the relative readout intensity. (b) Retrieved pulse energy (normalized to that at zero detuning) as a function of $\omega_s - \omega_l - \omega_m$ and with a relative readout intensity of 1 (blue squares) and 0.45 (black circles). The red dotted lines in (a) and (b) show the theoretical calculations with all parameters taken from the experiment. (c) Theoretically calculated temporal profile of the signal and retrieved pulses, along with the intensity of the stored mechanical oscillation (dotted line), with all parameters taken from the experiment in Fig. 2(a). The inset shows the calculated spatial displacement pattern of the (1, 2) mechanical mode.

between the readout and writing pulses is nearly twice the mechanical lifetime.

The signal-to-retrieval conversion efficiency shown in Fig. 2(a) is also limited by the relatively large cavity decay rate of the deformed silica resonator. Near unity conversion efficiency can be realized with $G \gg (\gamma_m, \kappa)$, which is achievable with nondeformed silica resonators that feature ultrahigh optical finesse. For the coupled oscillator system, the mapping between an optical pulse and a mechanical excitation is governed by the optomechanical pulse area defined as $\theta(t) = \int dt G(t)$ [22]. In the absence of any damping, perfect mapping occurs with $\pi/2$ writing and readout pulses. The theoretical calculation shown in Fig. 1(c), which is obtained with $\pi/2$ writing and readout pulses and with $\kappa/2\pi = 0.5$ MHz, $\gamma_m/2\pi = 10$ kHz, and $G_0/2\pi = 2$ MHz, features a much greater conversion efficiency than that in Fig. 3(c). For our experiments with $\kappa \gg G \gg \gamma_m$, the conversion efficiency continues to rise as the pulse areas exceed $\pi/2$, but eventually saturates, leading to the observed nonlinear dependence on the intensities of the writing and readout pulses. As shown in Fig. 3(a), the observed dependence of the retrieved pulse energy on the readout intensity is well described by the theoretical calculation. Similar behaviors have also been obtained for the dependence on the intensity of the writing pulse.

The optomechanical storage process is closely related to EIT, but with the coherent coupling between the signal field and the mechanical displacement controlled by the optomechanical area of the writing pulse. The optomechanical retrieval process is closely related to optomechanical laser cooling. For the retrieval process, the readout laser pulse couples to the stored mechanical excitation, transferring or damping the mechanical excitation to generate the retrieved pulse, as shown in Figs. 1(c) and 3(c).

Figure 3(b) plots as the dotted curve the theoretically calculated retrieved pulse energy as a function of $\omega_s - \omega_l - \omega_m$. The theoretical spectral line shape is in good agreement with the experiment. Additional calculations show that the observed spectral linewidth in Fig. 3(b) is primarily due to the finite duration of the signal and writing pulses (see [26]).

It should be noted that while the quantum state of a single optical mode can in principle be stored in a mechanical mode [22], the long-lived mechanical excitation generated in the storage process does not contain information on the spatial-temporal profile of the optical pulse. Although the manifestation of EIT in optical transmission is the same for both atomic and optomechanical systems, spatially extended excitations similar to dark-state polaritons in atomic media cannot be formed in a single optomechanical resonator [27]. The optical signal pulse, however, can in principle be localized, and its spatial-temporal profile be stored in an array of optomechanical resonators via processes analogous to those used in dynamically tunable coupled-resonator optical waveguides [7], as proposed recently [28]. In contrast to an all-optical system, optical properties of an optomechanical system can be effectively controlled with optical pulses via radiation pressure.

In summary, by exploiting transient optomechanical processes, we have successfully demonstrated optomechanical light storage in a silica resonator, with the storage lifetime determined by the mechanical damping time. At room temperature, thermal excitation of the mechanical oscillator leads to a thermal background in the storage and retrieval processes, which is negligible for most classical applications, but prevents the application of the optomechanical light storage in a quantum regime. Recent experimental efforts have successfully cooled mechanical oscillators to their quantum ground state [29–31], or near their quantum ground state [32]. Together with these latest advances, the demonstration of optomechanical light storage opens up exciting opportunities for exploring unique properties of optomechanical systems in applications including quantum memory and quantum optical wavelength conversion.

This work is supported by the DARPA-MTO ORCHID program through a grant from AFOSR.

[1] R. S. Tucker, P. C. Ku, and C. Chang-Hasnain, Electron. Lett. **41**, 208 (2005).
[2] H. J. Briegel *et al.*, Phys. Rev. Lett. **81**, 5932 (1998).
[3] H. Lin, T. Wang, and T. W. Mossberg, Opt. Lett. **20**, 1658 (1995).
[4] C. Liu *et al.*, Nature (London) **409**, 490 (2001).
[5] D. F. Phillips *et al.*, Phys. Rev. Lett. **86**, 783 (2001).
[6] K. Hammerer, A. S. Sorensen, and E. S. Polzik, Rev. Mod. Phys. **82**, 1041 (2010).
[7] M. F. Yanik and S. H. Fan, Phys. Rev. Lett. **92**, 083901 (2004).
[8] Q. F. Xu, P. Dong, and M. Lipson, Nature Phys. **3**, 406 (2007).
[9] T. Baba, Nat. Photon. **2**, 465 (2008).
[10] Z. M. Zhu, D. J. Gauthier, and R. W. Boyd, Science **318**, 1748 (2007).
[11] T. J. Kippenberg and K. J. Vahala, Science **321**, 1172 (2008).
[12] T. J. Kippenberg *et al.*, Phys. Rev. Lett. **95**, 033901 (2005).
[13] O. Arcizet *et al.*, Nature (London) **444**, 71 (2006).
[14] S. Gigan *et al.*, Nature (London) **444**, 67 (2006).
[15] A. Schliesser *et al.*, Phys. Rev. Lett. **97**, 243905 (2006).
[16] J. D. Thompson *et al.*, Nature (London) **452**, 900 (2008).
[17] S. Groblacher *et al.*, Nature (London) **460**, 724 (2009).
[18] Y. S. Park and H. L. Wang, Nature Phys. **5**, 489 (2009).
[19] S. Weis *et al.*, Science **330**, 1520 (2010).
[20] J. D. Teufel *et al.*, Nature (London) **471**, 204 (2011).
[21] A. H. Safavi-Naeini *et al.*, Nature (London) **472**, 69 (2011).
[22] L. Tian and H. L. Wang, Phys. Rev. A **82**, 053806 (2010).
[23] K. Stannigel *et al.*, Phys. Rev. Lett. **105**, 220501 (2010).

[24] A. H. Safavi-Naeini and O. Painter, New J. Phys. **13**, 013017 (2011).
[25] C. A. Regal and K. W. Lehnert, J. Phys. Conf. Ser. **264**, 012025 (2011).
[26] See Supplemental Material at http://link.aps.org/supplemental/10.1103/PhysRevLett.107.133601 for details of theoretical models, sample fabrication, experimental setup, and time-gated heterodyne detection.
[27] M. Fleischhauer and M. D. Lukin, Phys. Rev. Lett. **84**, 5094 (2000).
[28] D. E. Chang *et al.*, New J. Phys. **13**, 023003 (2011).
[29] A. D. O'Connell *et al.*, Nature (London) **464**, 697 (2010).
[30] J. D. Teufel *et al.*, Nature (London) **475**, 359 (2011).
[31] J. Chan *et al.*, arXiv:1106.3614.
[32] R. Riviere *et al.*, Phys. Rev. A **83**, 063835 (2011).